Title
Ongoing dynamics in large-scale functional connectivity predict perception

Journal
Proceedings of the National Academy of Sciences of the United States of America, 112(27)

ISSN
0027-8424

Authors
Sadaghiani, Sepideh
Poline, Jean-Baptiste
Kleinschmidt, Andreas
et al.

Publication Date
2015-07-07

DOI
10.1073/pnas.1420687112

Peer reviewed

Ongoing dynamics in large-scale functional connectivity predict perception

Sepideh Sadaghiani[a,1], Jean-Baptiste Poline[a,b], Andreas Kleinschmidt[c], and Mark D'Esposito[a,b,d]

[a]Helen Wills Neuroscience Institute, University of California, Berkeley, CA 94720; [b]Henry H. Wheeler Jr. Brain Imaging Center, University of California, Berkeley, CA 94720; [c]Department of Clinical Neurosciences, University Hospital and University of Geneva, 1211 Geneva, Switzerland; and [d]Department of Psychology, University of California, Berkeley, CA 94720

Edited by Robert Desimone, Massachusetts Institute of Technology, Cambridge, MA, and approved June 3, 2015 (received for review November 4, 2014)

Most brain activity occurs in an ongoing manner not directly locked to external events or stimuli. Regional ongoing activity fluctuates in unison with some brain regions but not others, and the degree of long-range coupling is called functional connectivity, often measured with correlation. Strength and spatial distributions of functional connectivity dynamically change in an ongoing manner over seconds to minutes, even when the external environment is held constant. Direct evidence for any behavioral relevance of these continuous large-scale dynamics has been limited. Here, we investigated whether ongoing changes in baseline functional connectivity correlate with perception. In a continuous auditory detection task, participants perceived the target sound in roughly one-half of the trials. Very long (22–40 s) interstimulus intervals permitted investigation of baseline connectivity unaffected by preceding evoked responses. Using multivariate classification, we observed that functional connectivity before the target predicted whether it was heard or missed. Using graph theoretical measures, we characterized the difference in functional connectivity between states that lead to hits vs. misses. Before misses compared with hits and task-free rest, connectivity showed reduced modularity, a measure of integrity of modular network structure. This effect was strongest in the default mode and visual networks and caused by both reduced within-network connectivity and enhanced across-network connections before misses. The relation of behavior to prestimulus connectivity was dissociable from that of prestimulus activity amplitudes. In conclusion, moment to moment dynamic changes in baseline functional connectivity may shape subsequent behavioral performance. A highly modular network structure seems beneficial to perceptual efficiency.

functional connectivity | brain networks | dynamics | graph theory | classification

The brain is highly active in a continuous manner, and much of neural activity is not directly locked to external events or stimuli. This continuous brain activity is spatiotemporally organized into a functional connectivity architecture that comprises several large-scale networks. Large-scale networks span different cerebral lobes and include subcortical structures (1). The regions comprised in such networks commonly coactivate together in response to task demands (2), but they also show correlated and spontaneous activity fluctuations when no changes occur in the external environment. The functional connectivity architecture ensuing from these activity cofluctuations largely persists across all mental states, including various tasks, resting wakefulness, and sleep, albeit showing some degree of modulation across these states (3, 4).

Strength and spatial distributions of functional connectivity within this architecture are not, however, stationary across time. At the spatial level of large-scale networks, functional connectivity shows prominent changes over the range of seconds to minutes (5). These so-called infraslow timescales and the spatial distribution of large-scale networks can be particularly well-investigated using functional MRI (fMRI). We refer to the nonstationarity of functional connectivity as ongoing dynamics. The notion of ongoing refers to dynamics that are not brought about by particular external events, such as stimuli or cues. Such large-scale ongoing network dynamics are thought to be crucial for the brain to explore a large space of dynamic functional capabilities (6). This potential functional importance has recently sparked interest in ongoing connectivity dynamics (5). The most common approach to studying ongoing dynamics in connectivity with fMRI has been to measure connectivity in time windows sliding through a prolonged task-free resting state (reviewed in ref. 5). These investigations have established the nonstationarity of large-scale functional connectivity that previously had been largely neglected. Some studies have shown characteristic changes of dynamic connectivity in different patient populations (7). However, none of these resting-state studies have directly investigated the functional consequences of ongoing dynamics during performance (in other words, how moment to moment changes in baseline functional connectivity relate to cognition and behavior). Furthermore, the ongoing dynamics of functional connectivity may be modulated by cognitive task context, further motivating investigation of the behavioral importance during task beyond the resting state.

Several lines of research call for a dedicated investigation of this question. Slow ongoing fluctuations in regional prestimulus baseline activity amplitudes (in fMRI or electrophysiological recordings) in task-relevant sensory or motor regions (8–12) as well as entire large-scale brain networks (12–14) correlate with evoked neural response strength and subsequent behavior. It is not clear whether, beyond fluctuations in regional ongoing activity amplitude, the correlation of such amplitude fluctuations across large-scale network regions (i.e., connectivity) relates to behavioral variability. Some prior work seems to suggest that ongoing connectivity dynamics between two task-relevant regions may turn behaviorally relevant (15). Also, in addition to these effects in infraslow timescales, some electrophysiological recordings indicate a behavioral relevance for phase synchrony between individual regions of interest and the rest of the brain at faster

Significance

Most brain activity is not directly evoked by specific external events. This ongoing activity is correlated across distant brain regions within large-scale networks. This correlation or functional connectivity may reflect communication across brain regions. Strength and spatial organization of functional connectivity changes dynamically over seconds to minutes. Using functional MRI, we show that these ongoing changes correlate with behavior. The connectivity state before playback of a faint sound predicted whether the participant was going to perceive the sound on that trial. Connectivity states preceding missed sounds showed weakened modular structure, in which connectivity was more random and less organized across brain regions. These findings suggest that ongoing brain connectivity dynamics contribute to explaining behavioral variability.

Author contributions: S.S., A.K., and M.D. designed research; S.S. performed research; S.S. and J.-B.P. analyzed data; and S.S., A.K., and M.D. wrote the paper.

The authors declare no conflict of interest.

This article is a PNAS Direct Submission.

[1]To whom correspondence should be addressed. Email: sepideh.sadaghiani@gmail.com.

This article contains supporting information online at www.pnas.org/lookup/suppl/doi:10.1073/pnas.1420687112/-/DCSupplemental.

timescales (16). Building on this so-far rather sparse evidence, we here sought to investigate behavioral effects from ongoing dynamics in large-scale functional connectivity, calling on tools of multivariate classification for trial by trial prediction of behavior and graph theory for a more detailed and spatially comprehensive characterization.

We analyzed behavioral outcome on a trial by trial basis as a function of dynamic connectivity states before stimulus presentation. We tested whether large-scale functional connectivity states predict perception of a sparse and irregularly appearing stimulus. To investigate ongoing nontask-locked changes in baseline connectivity, we minimized contributions from stimulus-evoked activity. This study, therefore, extends beyond important previous investigations of connectivity dynamics that occur after changes in the external environment (such as stimulation, cues, instructions, or feedback) at infraslow (17–20) and fast electrophysiological timescales (21, 22). Specifically, we asked (*i*) whether ongoing dynamics of large-scale functional connectivity relate to perceptual performance and (*ii*) which properties of baseline functional connectivity distinguish brain states that support perceptual accuracy from those that do not.

Eleven blindfolded participants performed a detection task on an auditory broadband stimulus (500 ms). They pressed a button whenever they heard the sound during two to three 20-min-long fMRI runs. The stimulus was presented at the individually determined detection threshold and repeated very sparsely at highly variable interstimulus intervals ranging from 20 to 40 s (Fig. 1*A*). This dataset has previously been used to investigate behavioral correlates of baseline activity amplitudes and enables this investigation to directly compare effects from prestimulus activity amplitudes with those from prestimulus connectivity (12). The unusually long interstimulus interval design allowed us to focus all analyses on the prestimulus time after excluding the hemodynamic response evoked by the previous stimulus. To answer our first question of whether prestimulus baseline connectivity predicts behavior, we applied trial by trial classification of subsequent perceptual outcome based on patterns of functional connectivity before stimulus presentation. To address our second question and determine what characterizes the difference across these brain states, we modeled connectivity before hits and before misses as separate graphs using tools of complex network theory and compared graph metrics between these states.

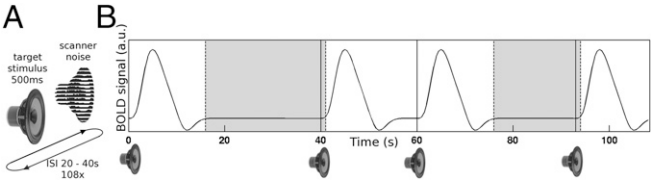

Fig. 1. (*A*) Experimental design of a threshold-level auditory stimulus presented on top of background scanner noise at very long, unpredictable interstimulus intervals (ISI, 20–40 s). Participants listened for the faint target sound continuously throughout 20-min runs and pressed a response button whenever they perceived the target. (*B*) Illustration of baseline time segments unaffected by evoked responses that were defined as appropriate for analysis of ongoing functional connectivity (marked in gray). The illustrated blood-oxygen-level-dependent (BOLD) hemodynamic response peaks at 6 s, reaches maximum poststimulus undershoot at 12 s, and returns to baseline before 16 s relative to stimulus onset according to finite impulse response estimation of the brain response to this stimulus in the same data in 10 bilateral brain areas (12). Baseline segments started after 16 s poststimulus and ended 1 s after the next stimulus onset. Baseline segments shorter than 6 s in length (interstimulus interval <22 s) were excluded. For classification analyses requiring trial by trial data, data were further restricted to baseline segments that were at least 15 s long (10 image volumes and interstimulus intervals ≥31 s). In this exemplary 2-min period of the task, four stimuli (marked as solid vertical lines) occur at interstimulus intervals of 40 (maximum in this design), 20 (minimum), and 32 s. Note that, for simplification, this illustration does not depict the spontaneous signal fluctuations during the baseline period and the ensuing variability in stimulus-evoked hemodynamic responses that are at the heart of this study.

Results

Overall, the threshold stimulus was detected in slightly more than one-half of the trials (62.2% ± 17% hits; defined as a button press within 1.5 s of stimulus onset). Perceptual outcome (hit vs. miss) was approximately stochastically distributed and independent of preceding interstimulus interval length (12).

Fig. 1 illustrates the selection of time segments of fMRI signal that were expected to be unaffected by any evoked activity. This procedure resulted in 26.5 ± 12.4 baseline segments (on average, 13.3 ± 2.25 volumes per segment) before hits and 15.6 ± 8.7 baseline segments (13.6 ± 2.56 volumes per segment) before misses per participant. For these time segments, we extracted fMRI signal from 24 regions of interest. These regions were defined on a participant by participant basis using seed-based resting-state functional connectivity on a task-free session (20 min) recorded on an earlier day and a passive functional auditory localizer. They were chosen in accord with our previous work on prestimulus activity, thereby making the investigations directly comparable (*SI Text*, section 1).

Prestimulus Baseline Connectivity Pattern. To explore the difference in connectivity before hits (pre-hits) and before misses (pre-misses), prestimulus baseline segments (last four volumes) were concatenated across all hits and across all misses for each participant. The difference in within-network connectivity was investigated in the networks where we previously found behaviorally relevant differences in prestimulus activity amplitudes (12): auditory (AUD), cinguloopercular (CO), frontoparietal (FP), default mode (DM), and dorsal attention (DAT) networks. To this end, the correlations were averaged from all region pairs within each network and entered into a two-way ANOVA of network (AUD, CO, FP, DAT, and DM) and condition (pre-hits and pre-misses). These within-network average correlations showed a significant interaction ($F_{2.9,29.1} = 3.33$, $P = 0.034$), and a two-sided posthoc t test was significant only in the DM network (stronger within-network connectivity for pre-hits $t_{10} = 3.72$, $P = 0.004$).

We further investigated whether coupling of the task-relevant AUD network with the other networks differed before hits and misses. Correlations were averaged across all of the respective region pairs. We found an interaction of condition (pre-hits and pre-misses) and network (CO, FP, DAT, and DM): $F_{2.6,26.2} = 4.31$, $P = 0.017$. Two-sided posthoc t tests were significant for AUD–CO connectivity ($t_{10} = 3.01$, $P = 0.013$) and AUD–DM connectivity ($t_{10} = -3.02$, $P = 0.013$). Before hits, auditory cortex showed stronger coupling with the CO network but decreased coupling with the DM network. These effects persisted after equating the number of image volumes across pre-hits and pre-misses (*SI Text*, section 2 and Fig. S1). For a fine-grained visualization, the group-level contrast between the full 24 × 24 correlation matrices for pre-hits and pre-misses is shown in Fig. 2*B*. For comparison, we generated the equivalent figure after concatenating baseline segments according to the previous rather than the upcoming percept. This procedure resulted in a very distinct pattern (*SI Text*, section 3 and Fig. S2), indicating that the difference structure observed in Fig. 2*B* was not substantially driven by preceding evoked activity fluctuations.

Classification of Upcoming Percept. To address whether dynamic changes in ongoing functional connectivity influence perceptual decisions, we attempted to predict the upcoming percept from trial by trial prestimulus connectivity. The univariate contrast in prestimulus connectivity described above was used for feature selection in subsequent classification analyses (compare with Fig. 2*B*). A naïve Bayesian classifier predicted the upcoming percept significantly above permutation chance level ($z = 2.30$, $P = 0.011$; 62.5% correct) (Fig. 3*A*). Note that chance level was 58.6% rather than 50%, because Bayesian classifiers take advantage of the prior probability of hits being more common than misses. Using a linear classifier resulted in a 50.5% chance level and again, produced significant above-chance classification performance (56.0% correct; $z = 2.36$, $P = 0.009$). Training the naïve

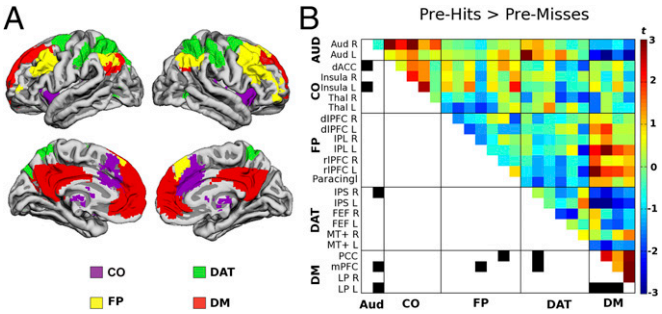

Fig. 2. (*A*) Intrinsic functional connectivity networks derived from seed-based correlations in an independent resting-state session (12). (*B*) Difference in cross-correlation for pre-hits > pre-misses. Each data point corresponds to a paired *t* test (uncorrected) between the two respective regions. Connections passing $P < 0.02$ (uncorrected) are marked in black in the lower triangle of the matrix to exemplify the features used for subsequent classification analyses (from similar difference matrices leaving one trial out) (*Methods*). Of note, all 12 connections corresponded to connectivity with DM or AUD networks. dACC, dorsal anterior cingulate cortex; dlPFC, dorsolateral prefrontal cortex; FEF, frontal eye fields; IPL, inferior parietal cortex; IPS, intraparietal sulcus; L, left; LP, posterior lateral parietal cortex; mPFC: medial prefrontal cortex; MT+: middle temporal area; Paracingl, paracingulate cortex; PCC, posterior cingulate/precuneus; R, right; rlPFC, rostrolateral prefrontal cortex; Thal, thalamus.

Bayesian classifier on upcoming percepts as described above but testing it on the previous rather than the next percept performed at chance level ($P = 0.68$), indicating that classification was not substantially driven by residual activity from the preceding trial.

Next, we investigated whether prestimulus functional connectivity contains predictive information over and above that reflected in prestimulus regional activity amplitudes. In line with our previous observation of behavioral relevance of prestimulus activity amplitudes (12), *N*aïve Bayesian classification on baseline activity amplitudes successfully predicted the upcoming percept ($z = 2.33$, $P = 0.010$; 60.8% vs. chance 56.1%) (Fig. 3*B*). We next asked whether adding prestimulus connectivity features to this classifier would further improve classification performance. The performance of a classifier will not increase substantially if additional features are included that do not add new, nonredundant information, even if the added features on their own have discrimination power (*SI Text*, section 4 and Fig. S3). When trained on the combination of prestimulus activity amplitudes and connectivity features, the classifier predicted the upcoming perceptual decision with substantially higher precision of $z = 3.87$ ($P = 0.00005$; 63.6% vs. chance 55.4%) (Fig. 3*C*) than using prestimulus activity amplitudes alone. A power analysis of classification success (*SI Text*, section 5) found powers of 0.67 for prestimulus connectivity, 0.73 for prestimulus activity amplitudes, and 0.98 for combined activity amplitudes and connectivity. This improvement indicates that baseline connectivity is of relevance for perception over and above the effect of activity levels per se.

Graph Theoretical Characterization of a Brain State Supporting Perceptual Accuracy. After showing that functional connectivity differs before hits vs. misses, we next sought to identify characteristics of this difference. To quantify these characteristics at the whole-brain level, we applied complex network or graph theory. This approach models the brain as a graph, with regions represented as nodes and functional connections represented as edges between them. Functional brain networks emerge as modules of highly interconnected nodes, with relatively few long-distance edges integrating across modules. This topologically modular organization is characteristic of the brain and other complex systems and enables flexible behavior based on specialized processes in locally segregated modules as well as more globally integrated functions through fast communication across modules (23). The strength of modular organization can be quantified using the modularity metric. In a brain state with high modularity, many modules (networks) have a high number of within-module compared with between-module connections.

For this complex network analysis, we used a more comprehensive and fine-grained set of 238 atlas regions (Fig. 4*A*) (1), because the modularity metric is likely to be better estimated with a larger number of nodes. For each participant and condition (resting state, pre-hits, and pre-misses), a single 238 × 238 correlation matrix was generated from time courses concatenated across all respective baseline segments (last four volumes per segment). For the resting-state session, baseline segments were defined from pseudotrials generated according to the same timing parameters as the task session. Next, an adjacency matrix was derived by thresholding the correlation matrices, resulting in unweighted, undirected graphs.

In Fig. 2*B*, we had observed that, across pre-hits and pre-misses, connectivity changes more consistently within networks (modules) and across pairs of networks than across random pairs of regions, suggesting that dynamical shifts in the modular structure may relate to behavioral outcome. We chose Newman's modularity (*SI Text*, section 8) to quantify such changes of modular integrity at the whole-brain level, because this metric provides a summary measure of within-module connectivity strength in relation to connectivity strength to other modules. In previous studies, modularity during the task-free resting state has been reported as a whole brain-level predictor for (offline) behavioral efficiency (24) and shown to describe modular network integrity in brain lesion patients (25). These observations of a role of modularity in interindividual variability further motivate investigation of this measure in intraindividual variability. In the first analysis, we assigned each node to one module according to the modular partition structure from ref. 1 as color-coded in Fig. 4*A*. We then tested for differences in modularity across conditions. Graph modularity was decreased before misses compared with hits (mean across costs: $t = 2.84$, $P = 0.027$ against permutation chance; Bonferroni-adjusted for three comparisons across condition pairs). This effect was also consistently observed for all individual costs ($P < 0.05$). Modularity before misses was likewise reduced compared with the task-free resting state ($t = 2.41$, $P = 0.033$, Bonferroni-adjusted). Conversely, pre-hits baseline showed no change in modularity compared with resting state ($t = 0.35$) (Fig. 4*D*). We replicated these effects after equating the number of imaging volumes across conditions (*SI Text*, section 2). Furthermore, we

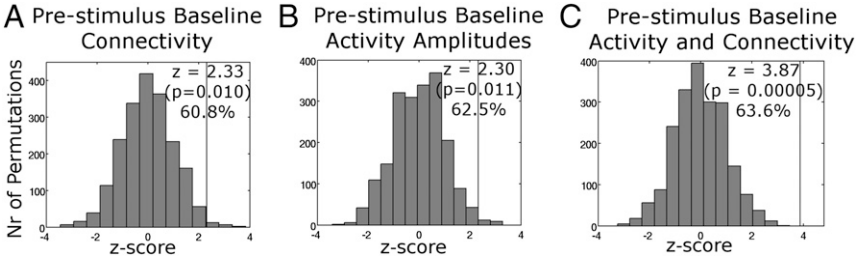

Fig. 3. Naïve Bayesian classifier performance (vertical line) and permutation distribution when trained on (*A*) prestimulus baseline connectivity, (*B*) prestimulus baseline activity amplitudes, and (*C*) the combination of prestimulus baseline activity amplitude and connectivity features. When trained on the combination of prestimulus activity and connectivity features, the classifier predicted the upcoming percepts with substantially higher precision than using prestimulus activity alone.

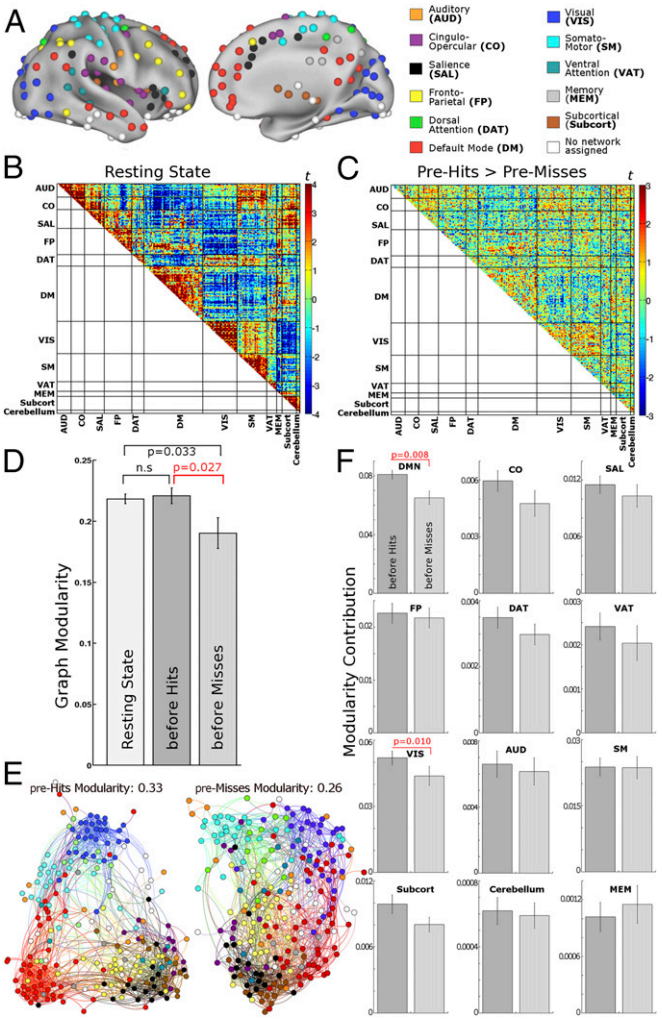

Fig. 4. Graph construction and graph modularity. (*A*) Nodes from a functional atlas defined on the combined basis of resting-state functional connectivity and a meta-analysis of cognitive tasks (1). (*B*) Resting-state correlation pattern across the nodes. This pattern with strong connectivity within the atlas modules shows that the predefined modular partition structure of the atlas reflects the data structure well. (*C*) Difference in functional connectivity of pre-hits baseline > pre-misses baseline (compare with Fig. 2*B*). Difference between task and resting state is in *SI Text*, section 7 and Fig. S5. (*D*) Graph modularity was reduced before misses compared with hits and task-free resting state. *P* values are Bonferroni-corrected. (*E*) A visual representation of the modularity difference before hits vs. misses for a representative individual participant (cost 0.05). This representation is generated by a force-field algorithm that treats nodes as magnets repulsing each other, whereas edges act as springs attracting the nodes that they connect (37). The configuration onto which these forces converge is visibly more modular before hits compared with misses. Networks (modules) are colored as in *A*. Most notably, DM (red) and VIS (dark blue) modules are less segregated from the rest of the graph before misses. (*F*) Contribution of individual modules to overall graph modularity. The strongest contribution to modularity difference was from DM and VIS networks. All error bars show SEMs. n.s., not significant.

confirmed the modularity difference using a graph partition derived from the participants' own resting-state data (*SI Text*, section 6 and Fig. S4). Finally, we investigated the most optimal modular partition structure as defined by maximizing modularity for each condition and participant separately. The spectral algorithm by Newman and Girvan (26) generated a modular partition for each graph as well as a modularity value for each graph (i.e., each participant and condition). This analysis confirmed a loss in modularity before misses compared with pre-hits ($t = 3.01$, $P = 0.027$) and the resting state ($t = 3.93$, $P = 0.005$). Pre-hits and resting state did not differ ($t = 2.06$; all Bonferroni-corrected for three comparisons). The number of modules showed no difference (pre-hits: 4.7 ± 0.8, pre-misses: 4.9 ± 0.7, and resting state: 4.7 ± 1).

Next, we investigated the contribution of each module to overall graph modularity, which is the sum of contributions from all individual modules. In a two-way ANOVA of modularity with factors condition (pre-hits and pre-misses) and module (12), a significant interaction ($F = 9.84$, $P = 0.008$) indicated that the modularity difference across perceptual outcomes differed across modules. Posthoc t tests were significant only in DM and visual (VIS) networks ($t = 3.23$, $P = 0.008$ and $t = 2.77$, $P = 0.010$), showing that the strongest contribution to the modularity difference across pre-hits vs. pre-misses originated from these networks (Fig. 4*F*). The observation in the DM network is in line with the significantly higher within-network connectivity during pre-hits baseline in this network (Fig. 2*B*).

We investigated nodal graph metrics to answer whether the decrease in modularity before misses was driven by a decrease in within-module connectivity, an increase of connectivity to other modules, or both. Within-module degree measures how strongly each node is interconnected within its own module, and participation coefficient quantifies each node's across-module connectivity (*SI Text*, section 8). We focused on DM and VIS networks, where the strongest modularity effect had been observed (Fig. 5 *A* and *B*). Within-module degree was significantly decreased before misses in both DM and VIS networks (average across the respective nodes and across five costs). This within-module degree decrease occurred across many but not all nodes of the graph (Fig. 5*C*), and the whole-brain average showed no significant difference (DM network: $t = 2.88$, $P = 0.03$; VIS network: $t = 3.01$, $P = 0.015$; whole brain: $t = 1.96$, not significant; *P* values Bonferroni-adjusted for three comparisons). Concurrently, participation coefficient was increased before misses in DM and VIS networks. Participation coefficient showed a universal pattern of decrease for pre-misses compared with pre-hits across the brain (Fig. 5*D*), and whole-brain average participation coefficient showed a significant effect (DM: $t = 3.43$, $P = 0.014$; VIS network: $t = 2.55$, $P = 0.045$; whole brain: $t = 3.67$, $P = 0.005$; Bonferroni-corrected for three comparisons). We replicated all within-module degree and participation coefficient results using the alternative graph partition that was derived from the participants' own resting-state data (*SI Text*, section 6).

Discussion

Our findings provide evidence that ongoing dynamic changes in the brain's large-scale connectivity structure correlate with behavior. In a threshold detection task, where perception of an identical stimulus varied from trial to trial, we observed that prestimulus baseline connectivity differed between hits and misses. Most notably, before misses, functional connectivity was lower between task-relevant auditory cortices and the CO network involved in the maintenance of tonic alertness (27, 28). Conversely, connectivity before misses was higher between auditory cortices and the DM network often observed to activate when the brain disengages from external cognitive demands (29) or engages in internal mentation (30). Furthermore, the DM network showed decreased within-network connectivity before misses compared with hits. Using graph theory metrics, a combination of reduced within-network connectivity and stronger connectivity to other networks was observed foremost in the DM as well as VIS networks before misses. Both of these networks could be considered noncritical for the auditory detection task. These observations may, therefore, indicate a behavioral advantage from encapsulation of networks not critical for the task at hand.

On a trial by trial basis, prestimulus baseline connectivity was predictive of perceptual outcome on subsequent stimulation. We observed that functional connectivity across large-scale networks estimated in single-trial, short (15–25 s) baseline time windows was informative enough to allow some classification of the

upcoming percept. Importantly, we made a particular effort to minimize the impact from evoked brain responses to the investigation of connectivity dynamics. Thus, our findings critically expand important previous fMRI investigations that used cue-evoked preparatory changes in connectivity for trial by trial prediction of behavior (17). Our results show that spontaneous, ongoing dynamics of brain connectivity are behaviorally relevant. Note that, in each classification cycle, all trials of all participants except for one trial entered the training set, and the classifier was tested on the left-out baseline segment. This procedure was chosen instead of the commonly used within-subject classification or leave one subject out procedures because of heterogeneity across participants and too few trials per participant (resulting from long interstimulus intervals). Because in general, the connectivity differences between individuals are much higher than between brain states within an individual, classifying across participants is difficult. However, our classifier's above-chance prediction performance indicates that there are connectivity dynamics consistent enough across the participants of this study to yield an informative common pattern. Fig. 2*B* confirms such a common pattern.

Modeling whole-brain connectivity states using graph theory, we found that, in the context of a simple perceptual task, higher modularity characterized a more efficient brain state for stimulus detection. When the modular segregation weakened and widespread communication across modules increased, the target sound was more likely to go undetected. This effect was expressed in both decreased within-module degree (each node's connectivity within its own module) in a variety of regions and widespread increase in across-module participation coefficient (each node's connectivity to other modules) before misses. These whole-brain results expand previous observations in prestimulus functional connectivity confined to task-relevant regions (15) or networks (19).

Finally, our data suggest that the behavioral relevance of connectivity dynamics goes beyond the sum of distributed amplitude fluctuations of regional brain activity. Trial by trial prediction of subsequent percepts improved when the classifier additionally used baseline connectivity patterns compared with baseline activity amplitudes alone. This observation indicates that baseline connectivity provides additional information. Furthermore, investigation of baseline connectivity revealed a pattern diverging from and informing beyond that of baseline activity amplitudes. For example, baseline activity amplitudes and connectivity did not always change in the same direction; whereas higher baseline activity amplitude in the VIS network was biasing toward missing the subsequent stimulus (12), higher baseline connectivity in this network was predictive of successful stimulus detection. Conversely, in the DM network, both prestimulus baseline activity (12) and baseline connectivity were higher before hits compared with misses. In summary, not only activity amplitude fluctuations but also, their interplay across regions are relevant for behavior.

Our findings raise the fundamental question of why the brain's processing architecture constantly undergoes such spatially extended modulations. In this auditory detection task, the behaviorally advantageous state showed only a limited and very specific increase of cross-module integration (e.g., between AUD and CO regions), whereas overall widespread integration was reduced. However, it is conceivable that, in more complex decision-making or working memory engagement, behavior would benefit from less modularity and hence, more widespread communication between task-relevant modules (e.g., see ref. 31 at much faster timescales). In other words, the brain may benefit from switching between states promoting locally integrated processing, e.g., for sensory perception, and states that integrate across modules to enable more complex cognition, albeit at the cost of modular tasks [see theoretical support for dynamic exploration of diverse intrinsic brain states (6) and the behavioral implications (32)]. In this context, it is important to note that ongoing dynamics in functional connectivity during cognitive task engagement may differ in strength and temporal and spatial

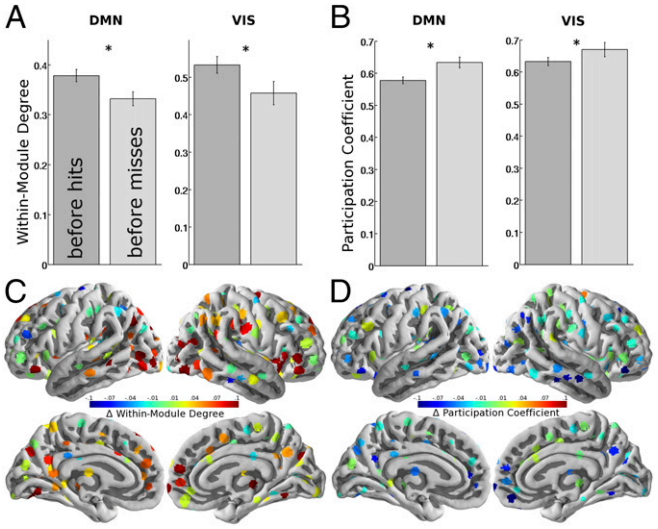

Fig. 5. Nodal graph measures. In both the DM and VIS networks, the previously observed loss of modularity before misses was driven by both (*A*) a decrease in within-network connectivity as measured by within-module degree and (*B*) an increase in across-network connectivity as measured by participation coefficient. Across the whole brain, decreases in modularity before misses coincided with (*C*) decreased within-module degree in many but not all nodes and (*D*) a more global tendency toward increased participation coefficient. Error bars show SEMs. *Significant at $P < 0.05$ after Bonferroni correction.

characteristics from the dynamics during resting state, although both share the important property of occurring without direct dependence on changes in the external environment. Characterization of such differences is an important question that requires in-depth investigation in dedicated studies. Although this complex question is beyond the scope of this study, an initial comparison in this dataset is provided in *SI Text*, section 7 and Figs. S5 and S6.

We conclude that spontaneous ongoing changes in baseline functional connectivity in and across large-scale brain networks correlate with perception and behavior. We found the dynamics in the strength of modular structure to be particularly important for behavior. Our analysis of large-scale connectivity captured functional connectivity dynamics occurring at infraslow timescales. Interestingly, behavioral performance when repeating the same task over and over again shows fluctuations with a qualitatively similar temporal profile as ongoing brain activity (i.e., high power at low frequencies; 1/frequency scale-free time history) (33). Although this temporal profile supports a strong relation between infraslow brain dynamics and behavioral variability, it likewise shows that behavior fluctuates as well at faster frequencies. The latter requires investigation of brain dynamics (in likely smaller networks) with methods allowing higher temporal resolution. Furthermore, our analyses could only capture dynamics that were consistent across trials of the same perceptual outcome (hits and misses) and across participants. However, functional connectivity dynamics are much more variable than observable in such dichotomous categorizations, with a wide-ranging repertoire of possible itinerant connectivity states. Importantly, however, in probing ongoing dynamic connectivity according to perceptual outcome, we were able to extract common characteristics of connectivity states that account for behavioral variability. Ongoing brain activity constitutes the vast majority of brain activity, and evoked responses add only a relatively small proportion (34). The findings obtained here, therefore, illustrate that any attempt to link behavior to brain function must conceptually integrate the role of ongoing brain activity and its connectivity dynamics.

NEUROSCIENCE

Methods

For paradigm, behavior, and fMRI data acquisition (3 Tesla, repetition time = 1.5 s) see ref. 12. Regions of interest (ROI) definitions are in *SI Text*, section 1.

Preprocessing and Head Motion. Standard preprocessing included realignment, coregistration, normalization and 5-mm FWHM spatial smoothing in SPM5. From each ROI's linearly detrended signal time course, we regressed out the estimated evoked response up to 24 s poststimulus for hits, misses, and false alarms using stick functions from the previously reported finite impulse response deconvolution (12). We regressed out as nuisance regressors global gray matter, white matter, cerebrospinal fluid, out-of-brain signals, and six linear head motion parameters.

To investigate the potential nonlinear impact of head motion, we calculated the number of motion outlier volumes using the derivative root mean square method (35) implemented in FSL (FMRIB). After trial by trial segmentation of the time courses (see below), the numbers of motion outliers per experimental run before hits (1.18 ± 1.53) vs. misses (0.85 ± 1.65) did not differ from each other ($P = 0.63$). Furthermore, the difference of graph metrics across pre-hits and pre-misses did not correlate with the difference in the number of head motion outliers across pre-hits and pre-misses over the participant group (modularity: $r^2 = 0.09$, $P = 0.37$; within-module degree: $r^2 = 0.1$, $P = 0.34$; participation coefficient: $r^2 = 0.002$, $P = 0.9$).

Baseline Time Segments. For classification analyses of activity amplitudes and connectivity requiring single-trial data, full baseline segments of 15 s or longer were used (292 hits and 172 misses across all participants) (Fig. 1). For all other analyses, only the last four volumes (6 s) before the next event were used from each segment of 6 s or longer, because the full baseline segment was not necessary for these analyses, and ongoing activity from the closest time points will have the strongest impact on the upcoming trial (cf. 12). These four-volume segments were concatenated across all hit trials (197 ± 71 volumes), all miss trials (129 ± 56.5), and all resting-state pseudotrials (160 volumes), yielding one correlation matrix per condition per participant.

Classification. For each single prestimulus baseline segment, Pearson cross-correlations (baseline connectivity classification) or mean signal amplitudes (baseline activity classification) entered classification. In each classification cycle, all data of all participants (464 trials), except for a single baseline segment, entered feature selection and the training set. The classifier was then tested on the left-out baseline segment. For baseline connectivity feature selection, the strongest 12 connections were selected from a 24×24 matrix expressing the difference of pre-hits vs. pre-misses connectivity as t values similar to those in Fig. 2*B* but generated leaving out the trial to be tested. For baseline activity, all 24 ROIs were used. Mean value across both categories (pre-hits and pre-misses) was removed for each feature and participant; $2{,}000 \times 464$ permutations of the training data labels gave the chance distribution.

Graph construction. Adjacency matrices were created for each participant from the Fisher-transformed Pearson cross-correlation matrices for pre-hits, pre-misses, and resting state thresholded at five cost values (fraction of strongest edges) to ensure that effects were not driven by particular connection density: 0.05, 0.1, 0.15, 0.2, and 0.25.

Graph metrics. Equations for modularity (26), within-module degree, and participation coefficient (36) are in *SI Text*, section 8.

Statistical hypothesis testing on graph metrics. Modularity, within-module degree, and participation coefficient cannot be assumed to be normally distributed. We, therefore, generated chance distributions for t and F values from 2,000 permutation cycles, where data from the different conditions (pre-hits and pre-misses) were randomized within each participant.

ACKNOWLEDGMENTS. We are thankful for insightful discussions with Gaël Varoquaux, Vincent Perlbarg, and Habib Benali on prestimulus connectivity; Jason Vytlacil on classification; and Maxwell Bertolero, Courtney Gallen, Caterina Gratton, and Robert White on graph theory. David L. Chang and Christopher E. Balcells supported analysis implementations. This work is supported by NIH Grants MH63901 and NS79698.

1. Power JD, et al. (2011) Functional network organization of the human brain. *Neuron* 72(4):665–678.
2. Smith SM, et al. (2009) Correspondence of the brain's functional architecture during activation and rest. *Proc Natl Acad Sci USA* 106(31):13040–13045.
3. Cole MW, Bassett DS, Power JD, Braver TS, Petersen SE (2014) Intrinsic and task-evoked network architectures of the human brain. *Neuron* 83(1):238–251.
4. Sadaghiani S, Hesselmann G, Friston KJ, Kleinschmidt A (2010) The relation of ongoing brain activity, evoked neural responses, and cognition. *Front Syst Neurosci* 4(20):20.
5. Hutchison RM, et al. (2013) Dynamic functional connectivity: Promise, issues, and interpretations. *Neuroimage* 80:360–378.
6. Deco G, Jirsa VK, McIntosh AR (2013) Resting brains never rest: Computational insights into potential cognitive architectures. *Trends Neurosci* 36(5):268–274.
7. Damaraju E, et al. (2014) Dynamic functional connectivity analysis reveals transient states of dysconnectivity in schizophrenia. *Neuroimage Clin* 5:298–308.
8. Fox MD, Snyder AZ, Vincent JL, Raichle ME (2007) Intrinsic fluctuations within cortical systems account for intertrial variability in human behavior. *Neuron* 56(1):171–184.
9. Hesselmann G, Kell CA, Kleinschmidt A (2008) Ongoing activity fluctuations in hMT+ bias the perception of coherent visual motion. *J Neurosci* 28(53):14481–14485.
10. Hesselmann G, Kell CA, Eger E, Kleinschmidt A (2008) Spontaneous local variations in ongoing neural activity bias perceptual decisions. *Proc Natl Acad Sci USA* 105(31): 10984–10989.
11. Monto S, Palva S, Voipio J, Palva JM (2008) Very slow EEG fluctuations predict the dynamics of stimulus detection and oscillation amplitudes in humans. *J Neurosci* 28(33):8268–8272.
12. Sadaghiani S, Hesselmann G, Kleinschmidt A (2009) Distributed and antagonistic contributions of ongoing activity fluctuations to auditory stimulus detection. *J Neurosci* 29(42):13410–13417.
13. Boly M, et al. (2007) Baseline brain activity fluctuations predict somatosensory perception in humans. *Proc Natl Acad Sci USA* 104(29):12187–12192.
14. Coste CP, Sadaghiani S, Friston KJ, Kleinschmidt A (2011) Ongoing brain activity fluctuations directly account for intertrial and indirectly for intersubject variability in Stroop task performance. *Cereb Cortex* 21(11):2612–2619.
15. Ploner M, Lee MC, Wiech K, Bingel U, Tracey I (2010) Prestimulus functional connectivity determines pain perception in humans. *Proc Natl Acad Sci USA* 107(1):355–360.
16. Keil J, Müller N, Hartmann T, Weisz N (2014) Prestimulus beta power and phase synchrony influence the sound-induced flash illusion. *Cereb Cortex* 24(5):1278–1288.
17. Ekman M, Derrfuss J, Tittgemeyer M, Fiebach CJ (2012) Predicting errors from reconfiguration patterns in human brain networks. *Proc Natl Acad Sci USA* 109(41): 16714–16719.
18. Sherwin JS, Muraskin J, Sajda P (2015) Pre-stimulus functional networks modulate task performance in time-pressured evidence gathering and decision-making. *Neuroimage* 111:513–525.
19. Thompson GJ, et al. (2013) Short-time windows of correlation between large-scale functional brain networks predict vigilance intraindividually and interindividually. *Hum Brain Mapp* 34(12):3280–3298.
20. Madhyastha TM, Askren MK, Boord P, Grabowski TJ (2015) Dynamic connectivity at rest predicts attention task performance. *Brain Connect* 5(1):45–59.
21. Supèr H, van der Togt C, Spekreijse H, Lamme VAF (2003) Internal state of monkey primary visual cortex (V1) predicts figure-ground perception. *J Neurosci* 23(8):3407–3414.
22. Weisz N, et al. (2014) Prestimulus oscillatory power and connectivity patterns predispose conscious somatosensory perception. *Proc Natl Acad Sci USA* 111(4):E417–E425.
23. Meunier D, Lambiotte R, Bullmore ET (2010) Modular and hierarchically modular organization of brain networks. *Front Neurosci* 4:200.
24. Stevens AA, Tappon SC, Garg A, Fair DA (2012) Functional brain network modularity captures inter- and intra-individual variation in working memory capacity. *PLoS ONE* 7(1):e30468.
25. Gratton C, Nomura EM, Pérez F, D'Esposito M (2012) Focal brain lesions to critical locations cause widespread disruption of the modular organization of the brain. *J Cogn Neurosci* 24(6):1275–1285.
26. Newman MEJ, Girvan M (2004) Finding and evaluating community structure in networks. *Phys Rev E Stat Nonlin Soft Matter Phys* 69(2 Pt 2):026113.
27. Sadaghiani S, et al. (2010) Intrinsic connectivity networks, alpha oscillations, and tonic alertness: A simultaneous electroencephalography/functional magnetic resonance imaging study. *J Neurosci* 30(30):10243–10250.
28. Sadaghiani S, D'Esposito M (April 25, 2014) Functional characterization of the cingulo-opercular network in the maintenance of tonic alertness. *Cereb Cortex*.
29. Gusnard DA, Raichle ME, Raichle ME (2001) Searching for a baseline: Functional imaging and the resting human brain. *Nat Rev Neurosci* 2(10):685–694.
30. Buckner RL, Carroll DC (2007) Self-projection and the brain. *Trends Cogn Sci* 11(2): 49–57.
31. Kitzbichler MG, Henson RNA, Smith ML, Nathan PJ, Bullmore ET (2011) Cognitive effort drives workspace configuration of human brain functional networks. *J Neurosci* 31(22):8259–8270.
32. Sadaghiani S, Kleinschmidt A (2013) Functional interactions between intrinsic brain activity and behavior. *Neuroimage* 80:379–386.
33. Gilden DL (2001) Cognitive emissions of 1/f noise. *Psychol Rev* 108(1):33–56.
34. Raichle ME (2009) A paradigm shift in functional brain imaging. *J Neurosci* 29(41): 12729–12734.
35. Power JD, Barnes KA, Snyder AZ, Schlaggar BL, Petersen SE (2012) Spurious but systematic correlations in functional connectivity MRI networks arise from subject motion. *Neuroimage* 59(3):2142–2154.
36. Guimerà R, Nunes Amaral LA (2005) Functional cartography of complex metabolic networks. *Nature* 433(7028):895–900.
37. Bastian M, Heymann S, Jacomy M (2009) Gephi: An open source software for exploring and manipulating networks. *Proceedings of the International AAAI Conference on Weblogs and Social Media*. Available at gephi.github.io/users/publications/.